

The Study on Data Hiding in Medical Images

Li-Chin Huang¹, Lin-Yu Tseng², and Min-Shiang Hwang³
 (Corresponding author: Min-Shiang Hwang)

Department of Computer Science and Engineering, National Chung Hsing University¹
 250, Kuo Kuang Rd., Taichung 402, Taiwan R.O.C.
 Department of Computer Science and Communication Engineering, Providence University²
 200, Chung-Chi Rd., Taichung 43301, Taiwan R.O.C.
 Department of Computer Science & Information Engineering Asia University³
 No. 500, Lioufeng Raod, Wufeng Shiang, Taichung, Taiwan, R.O.C.
 (Email: mshwang@asia.edu.tw)

(Received May 12, 2012; revised and accepted June 23, 2012)

Abstract

Reversible data hiding plays an important role in medical image systems. Many hospitals have already applied the electronic medical information in healthcare systems. Reversible data hiding is one of the feasible methodologies to protect the individual privacy and confidential information. With application in several high quality medical devices, the detection rate of diseases and treating are improved at the early stage. Its demands have been rising for recognizing complicated anatomical structures in high quality images. However, most data hiding methods are still applied in 8-bit depth medical images with 255 intensity levels. This paper summarizes the existing reversible data hiding algorithms and introduces basic knowledge in medical image.

Keywords: Difference expansion, histogram, medical image, reversible data embedding

1 Introduction

Over the Internet, many hospitals have already developed the electronic medical information to provide a better, safer, and more efficient healthcare. Medical information are digitized and transmitted among patients, medical professionals, health care providers, and institutes of medicine. For instance, electronic medical record (EMRs) will increase the accessibility and sharing of health records among authorized individuals. Such process is necessary for collecting private information during health care process since possible leaking of personal health information could result in significant economic, psychological, and social impairment to individuals. Furthermore, risks are rising due to usage of the Internet especially when illegal accessing and unauthorized tampering occurs. Therefore, data hiding in medical image is one of the feasible methodologies to protect the important information with authentication, fingerprinting, copy control, security, and covert communication.

Data hiding has recently been proposed as one of the promising techniques to embed secret data in cover images [23, 26, 27]. According to permanent distortion of the cover image, data hiding algorithms are divided into fragile data hiding and robust (semi-fragile) data hiding [15, 17]. The original images fail in restoration from stego-images because the cover images are distorted permanently. Therefore, these techniques do not satisfy the criteria for medical imaging systems, military imaging systems, remote sensing, law enforcement, and high precision systems in scientific research.

Recently, reversible data hiding, which is also called lossless data hiding, has been developed [1, 7, 12, 18]. Reversible data hiding can complete blind restoration of the original data from stego-images after retrieving the hidden data. There are three groups of reversible data hiding [11]: data compression [8], pixel-value difference expansion (DE) scheme [18], and histogram-based scheme [12].

Because of complex computation and limited capacity, data compression has more overhead than the other methods. In general, the data compression based reversible data hiding schemes are developed for images compressed by JPEG [5], vector quantization [25], and block truncation coding [6].

In 2003, Tian [22] developed DE method by integer wavelet transform. Tian examined the redundancy in digital images by expanding the difference between the two neighboring pixels pairs to obtain high-capacity and low-distortion. Based on DE method, Lou et al. [16] provide a multiple layer data hiding scheme for medical images.

Histogram shifting is an important technique applied in reversible data hiding. Vleeschouwet et al. [24] adopted circular interpretation of bijective transformations. In 2011, Luo et al. [14] proposed a preserving the medians of image block to improve the capacity of embedded secret data.

Data hiding is an important method to protect patient's

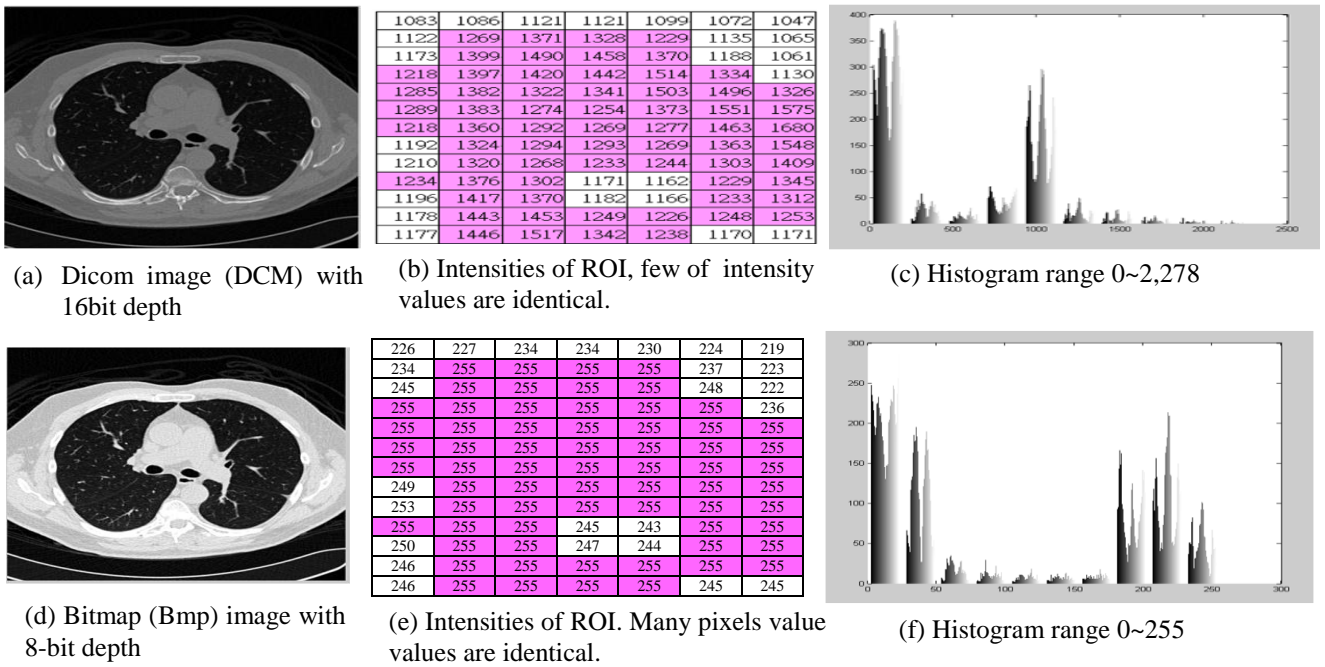


Figure 1: 16-bit depth and 8-bit depth in medical image

privacy in medical imaging systems. In 2011, Chang et al. [2] utilize repetitive pixels in a digital medical image to develop a reversible data embedding scheme without location map compression. Without restoration of the original medical image, some data hiding schemes [2, 10] can also provide preliminary diagnosis medical images. These kinds of data hiding schemes embed secret messages into the Region of Non-Interest (RONI) and a few pixels are embedded in the Region of Interest (ROI). For mobile healthcare applications, Rochan et al. [20] adopts arithmetic coding with cryptography to embedding data in a medical image. Fallahpour et al. [10] propose a gradual medical data insertion increased by doctor observations during diagnosis and treatment.

Although many algorithms [2, 12, 16, 21] have been proposed for medical imaging systems, most of them are still testing on 8-bit depth medical images which express intensity levels from 0 to 255. However, many high quality medical devices are adopted to improve the detection rate of diseases and treating at the early stage. Therefore, there are strong demands for recognizing complicated anatomical structures in images on high quality of medical images with 16-bit depth. Because 16-bit depth images have intensity 65,536 discrete levels, great precision of images is required to express the smooth surface of anatomical structures demonstrated, as shown in Figure 1. In 8-bit depth medical images, most of light anatomical structures are expressed by 255. However, 16-bit depth image demonstrates the light part of anatomical structures as a different intensity. Duplicated intensities will be demonstrated in 8-bit depth medical images since intensity ranges from 0 to 255. On the contrary, less duplicated intensity will appear in 16-bit depth to embed secret bits for data hiding, as shown in

Table 1: The comparison of 16-bit and 8-bit depth medical images

| Medical Image Type | 16-bit depth | 8-bit depth |
|-------------------------------|--------------|-------------|
| The Range of Intensity | 65,536 | 256 |
| Image Precision | High | Low |
| Duplicate Intensity | Less | More |
| Overflow Handling | Easy | Difficult |
| Underflow Handling | Easy | Difficult |
| Utilization Rate of Intensity | Low | High |

Table 1.

This paper is organized as follows: Section 2 introduces background knowledge. Section 3 summarizes the data hiding schemes methods. The conclusion is given in Section 4.

2 Background Knowledge

2.1 Medical Image Database and Tool

The role of medical imaging in science is expanding, and consequently, the requirement of appropriate image-archiving and image-sharing mechanisms is evolving. The Cancer Imaging Archive (TCIA) [19] is provided by the Cancer Imaging Program for any cancer research. TCIA provides a freely accessible, open archive of cancer-specific medical images and metadata accessible for public download from website.

Image J is a free, Java-based image processing program developed by the National Institutes of Health. Image J can display, edit, analyze, and process. Furthermore, it can read

many image formats including DICOM, JPEG, BMP, TIFF, and so on.

2.2 Digital Imaging Communications in Medicine (DICOM)

DICOM [9] is a standard for medical image data exchange such as handling, storing, printing, and transmitting information. This standard is managed by the National Electrical Manufacturers Association (NEMA). DICOM integrates manufactures of imaging equipment and imaging information systems such as film scanners, printers, computer monitors and workstations, and image archives. Matlab provides functions to operate DICOM medical images such as dicomread, dicomwrite, and dicominfo.

2.3 Salt-and-pepper Noise

Salt and pepper noises are typically seen on images presented by white and black pixels. In general, the salt-and-pepper has an extra peak at the white end of the spectrum since the noise components were pure black and white.

2.4 Overflow/Underflow Problem

Overflow/Underflow is the value of pixels exceeding the range of intensity levels in images. For instance, the overflow problem will happen if pixel values $I > 255$ are assigned to 8-bit depth images during data embedding. On the contrary, the underflow problem will occur when the pixel values are assigned $I < 0$.

2.5 Location map

To prevent overflow/underflow, a one-bit map will be

created as the location map to record the location of overflow/underflow pixels. The size of location map is the same as the original image. In other words, an image of 512×512 pixels will create a location map of 512×512 pixels. For the location map with secret messages embedded to image, many compressions are applied to location map, for example: run-length coding algorithm and arithmetic coding algorithm. However, method of location map will increase the complexity of data hiding. If a bad compression ratio is obtained in location map, capacities will be wasted to record overhead bit to deal with overflow/underflow.

2.6 Modulo-256 Additions

Vleeschouwer et al. prevent overflow/underflow problem to apply modulo-256 addition [24] in reversible data hiding. However, this technique has suffered from the annoying salt-and-pepper noise. In other words, a very bright pixel with a large gray scale value close to 255 will be possibly changed to a very dark pixel with a small gray scale value close to 0, and vice versa.

3 Data Hiding Schemes in Medical Images

In this section, we summarize the existing reversible data hiding algorithms. Most of schemes are histogram shifting methods because the operation is very simple and efficient.

3.1 Reversible and High-Capacity Data Hiding in Medical Image

In 2011, Fallahpour et al. [1] apply the histogram shifting to each block between the minimum and the maximum frequency, with the largest frequency having the maximum data hiding capacity. In histogram of non-overlapping medical image blocks, most of peak is located around some grey values and the rest of the spectrum is empty. The zeros (or minimum) and the peaks (maximum) of the block image histogram will be shifted to embed secret messages. The detail of algorithm is described as follows.

A. Embedding algorithm

- 1) The image is divided into N_b non-overlapping blocks. Repeat (2)-(4) for each image blocks.
- 2) Let n be the number of (peak, zero). The more the number of pairs, the worse the image quality is. Then, the following iterations are executed n times for $i = 1:n$.
- 3) For pair (p_i, z_i) the image block will be scanned.

There are two kinds of conditions for different $peak_i$ and $zero_i$. The details are described as follows.

- (a) $p_i > z_i$

For all intensity values of pixels located between $z_i + 1$ and p_i , $[z_i + 1, p_i]$, histogram shifts leftward by reducing intensity value to one. Therefore, a gap will be created at grey level p_i .

If embedding bits are '1', the $p_i - 1$ pixels value will increase by 1. Otherwise, the $p_i - 1$ pixels value will not be modified.

- (b) $p_i < z_i$

For all intensity values of pixels located between $p_i + 1$ and $z_i - 1$, $[p_i + 1, z_i - 1]$, histogram shifts rightward by increase intensity value by one. Thus, a gap at grey level $p_i + 1$ will be created. If embedding bits are '1', the p_i is increased by 1. Otherwise, the intensity will not be changed.

B. Detection algorithm

- 1) The image is divided into N_b non-overlapping blocks, same as embedding algorithm. For each image blocks, steps 2-3 are executed separately.
- 2) The following iterations are repeated n times. For $i = 1:n$.
- 4) For pair (p_i, z_i) of the image block, there are two kinds of conditions for different $peak_i$ and $zero_i$. The

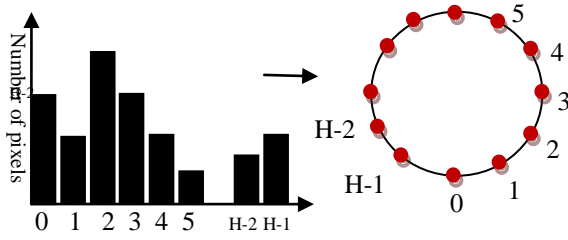


Figure 2: Histogram mapping onto a circle

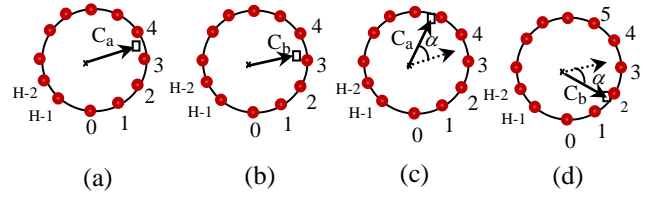


Figure 3: Embedding diagram of a data bit '1'

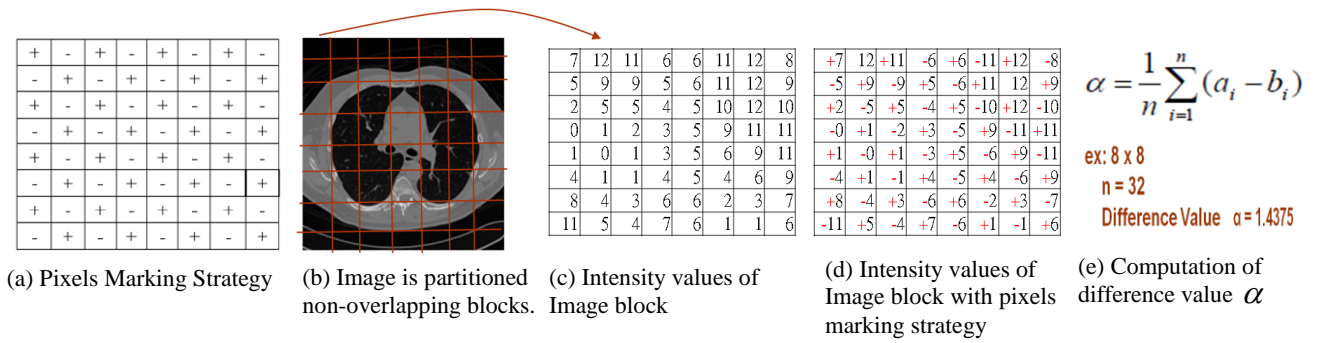


Figure 4: The pixels marking strategy is applied to non-overlapping image blocks with the difference value α computed

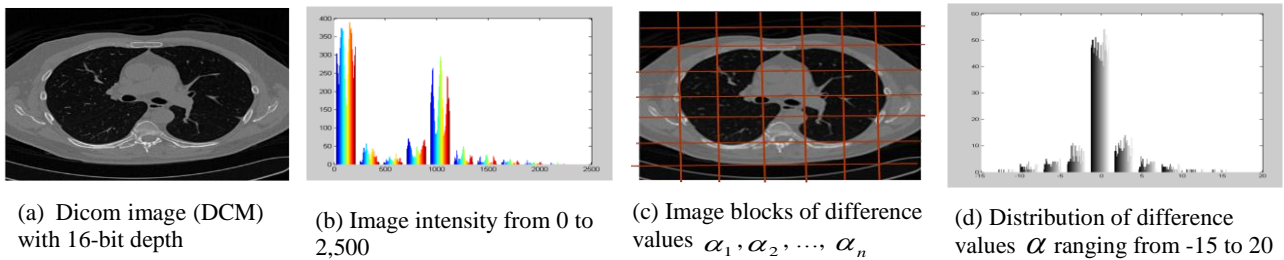


Figure 5: Distributions of image intensity and difference values α

details are described as follows.

(a) $p_i > z_i$

If the pixel value is p_i , the embedded data bit '1' will be extracted without changing histogram value. If the pixel value is $p_i - 1$, the embedded data bit '0' will be extracted and histogram shifts rightward with intensity value increased by 1. Then, all pixel value located between z_i and $p_i - 2$ will be increased by one.

(b) $z_i > p_i$

If the pixel value is p_i , the embedded data bit '0' will be extracted without modifying the histogram value. If the intensity value is $p_i + 1$, the embedded data bit '1' will be extracted with its intensity reduced by 1. Thus all pixel values located between $p_i + 2$ and z_i will be reduced by 1.

3.2 Data Hiding Method Based on Patchwork Theory

De Vleeschouwer et al. [24] applied the patchwork theory and modulo-256 addition to hiding data. The method is described as follows.

- 1) Each bit of the hidden data is associated with a group of pixels such as a block in an image. Each group is randomly separated into two sets of pixels zones A and B with the same size. The histogram of each zone is mapped to a circle shown in Figure 2. On the circle, each position is the corresponding grayscale values. And the weight of a position is the number of pixels at the corresponding grayscale value.
- 2) c_a and c_b vectors point to the mass center of zones A and B from the center of the circle, respectively. Zones A and B are two identical sets from the same block; therefore vectors c_a and c_b are similar to each other. This character is applied to embed secret messages. For instance, c_a rotates in clockwise direction and c_b rotates in counter-clockwise while embedding a bit "0". Similarly, c_a and c_b are respectively rotated in counter-clockwise and clockwise direction to embedding bit '1'. For example, two zones A and B

have the similar mass center of zones c_a and c_b . In

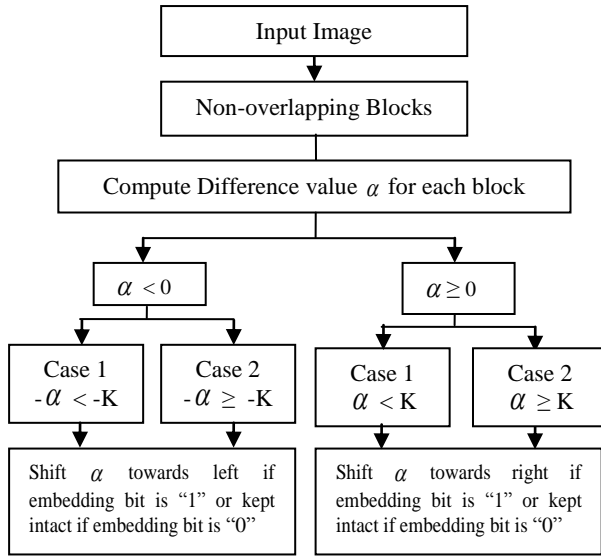


Figure 6: Bit embedding strategy

other words, c_a and c_b are located between 3 and 4, shown in Figure 3(a)(b). If embedding bit ‘1’, c_a and c_b are rotated in counter-clockwise and clockwise direction with angle. In other words, c_a and c_b have the 2 difference angles after embedding bit ‘1’, as demonstrated in Figure 3(d)(d).

3.3 Preserve Robustness for Image Data Hiding

Satre et al. [21] proposed a preserving robustness for image data hiding. In a local block, the pixel intensities are highly correlated with spatial redundancy. Therefore, image blocks of difference values are expected to be very close to zero, as shown in Figure 5. At the first stage, the image is partitioned into non-overlapping blocks such as 8×8 , 4×4 , and son. Furthermore, image blocks are partitioned into two sets A and B. All pixels in set A are marked by “+”, while all pixels in set B will be marked by “-“. Each image blocks are applied with pixels marking strategy to compute difference value as demonstrated in Figure 4. The difference value is computed as

$$\alpha = \frac{1}{n} \sum_{i=1}^n (a_i - b_i) \quad (1)$$

Where a_i is the pixel value marked by “+” and b_i is the pixel value marked by “-“. After the difference values α are obtained, the bit embedded strategy will be applied to embed secret messages. The details of data embedded and data extraction is described as follows.

A. Data embedding

The main idea of bit embedding is that the difference value located between threshold $-K$ and K embed bit “0” and the difference value α is shifted to beyond threshold K or $-K$

to embedded bit “1”. Therefore, there are two categories of embedding strategies as follows shown in Figure 6.

Category 1: $\alpha \geq 0$

Case 1: $0 \leq \alpha \leq K$

If the embedding bit is “1”, pixels in set A are shifted rightwards with distance K . If the embedding bit is “0”, pixels in set A are kept intact.

Case 2: $\alpha > K$

The embed bit is always “1” whether embedding bit is “0” or “1”. This will produce error bits in extraction stage. Therefore, BCH(63,7,15) will be applied to correction.

Category 2: $\alpha < 0$

Case 1: $-K \leq \alpha \leq 0$

If the embedding bit is “1”, pixels in set A are shifted leftwards with distance K . If the embedding bit is “0”, pixels in set A are kept intact.

Case 2: $\alpha \leq -K$

The embed bit is always “1” whether embedding bit is “0” or “1”. This will produce error bits in extraction stage. Therefore, BCH(63,7,15) will be applied to correction.

B. Data Extraction

Data extraction process is a reverse process of data embedding. Because case 2 of both categories can embed “0” or “1”, BCH code is applied to correct these errors.

3.4 Reversible Data Hiding Based on Block Median Preservation

In 2011 Luo et al. developed a block median preservation data hiding method. In order to extract secret messages and to restore original image correctly, the median pixel must be preserved i.e. its position is still accurately located during embedding and extraction stage. The detail of data embedding is shown in Figure 7.

A. Data embedding

Step 1. Image partition and subsampling.

The image I is partitioned a set of $u \times v$ blocks. At the same time, image I is also subsampled into subimages $s_1, s_2, \dots, s_{u \times v}$ with size $\lfloor \frac{W}{u} \rfloor \times \lfloor \frac{H}{v} \rfloor$.

Step 2. Median image computation

The sample values are sorted and the median position is defined as the median value of the subsample image. The median image will be constructed by each median value of subsample images. For instance, image I is subsampled into 4 subimages and $s_1(i, j) = 161, s_2(i, j) = 160, s_3(i, j) = 160, s_4(i, j) = 158$. Then the values of subimage are sorted as $s_4(i, j) = 158, s_2(i, j) = 160, s_3(i, j) = 160,$

$s_1(i, j) = 161$. The median of median value of the

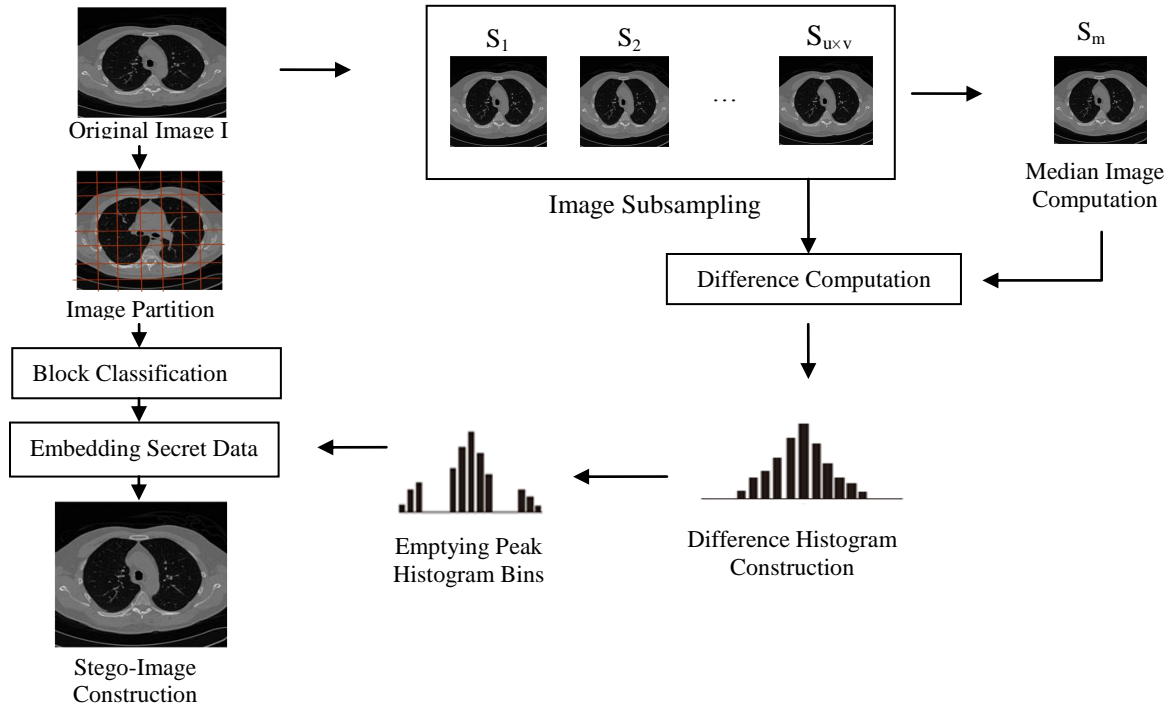


Figure 7: Block diagram of data embedding

subimage is $s_2(i, j) = 160$. All median values of the subimages will be constructed a median image shown in Figure 8.

Step 3. Block classification

Let n_l , n_0 , and n_r be the numbers of pixel values smaller, equal, and larger than median value $s_m(i, j)$. Then, $n_l + n_0 + n_r = u \times v$. According to the number of median values n_0 in subimages, the subimages are classified two types: Type I is $n_0 = 1$ and Type II is $n_0 \geq 2$. Furthermore, Type II is divided into three types by n_l and n_r . Therefore, Type II-1, Type II-2, and Type II-3 are represented by $n_l = n_r$, $n_l < n_r$, and $n_l > n_r$ separately.

Step 4. Difference computation

This step computes the difference between and $s_m(i, j), s_1, s_2, \dots, s_k$ where $1 \leq k \leq u \times v, k \neq m$.

Step 5. Difference histogram construction

All difference values from step 4 are constructed difference histogram.

Step 6. Empty peak points

The bins in the range of $[b_{-2EL-1}, b_{-EL-1}]$ and $[b_{EL+1}, b_{2EL+1}]$ are emptied. The formula is shown as follows.

$$d'_k(i, j) = \begin{cases} d_k(i, j) + EL & \text{if } d_k(i, j) > EL \\ d_k(i, j) - EL & \text{if } d_k(i, j) < -EL \\ d_k(i, j) & \text{otherwise} \end{cases} \quad (2)$$

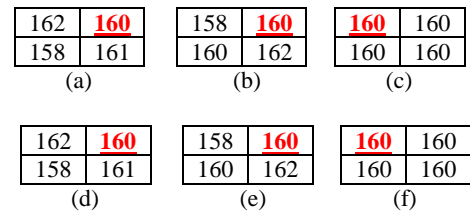


Figure 8: Examples of different 2×2 block types. (a) Type I, (b) and (c) Type II-1 and (e) Type II-2 (f) Type II-3.

Where $1 \leq k \leq u \times v, k \neq m$.

In case $EL = 2$, the bins smaller than b_{-2} and larger than b_2 are shifted leftward and rightward, respectively. Thus, $[b_{-5}, b_{-3}]$ and $[b_3, b_5]$ are emptied. The subimage blocks are also adjusted similarly as difference histogram. The formula as

$$s'_k(i, j) = \begin{cases} s_k(i, j) + EL & \text{if } d_k(i, j) > EL \\ s_k(i, j) - EL & \text{if } d_k(i, j) < -EL \\ s_k(i, j) & \text{otherwise} \end{cases} \quad (3)$$

where $1 \leq k \leq u \times v, k \neq m$.

Step 7. Histogram shifting

The strategy of histogram shifting depends on types of subsample. The detail is described as follows.

1) Type I

The secret bit is embedded by repeating $EL = 2$ and $EL = 1$ respectively, as shown in Figure 9(c)(d). The formula is described as follows.

$$s''_k(i, j) = \begin{cases} s'_k(i, j) + EL + w & \text{if } d_k(i, j) = EL \\ s'_k(i, j) - EL - w & \text{if } d_k(i, j) = -EL \end{cases} \quad (4)$$

where $1 \leq k \leq u \times v, k \neq m$.

2) Type II-1

If $EL > 0$, the secret bit is embedded by repeating $EL = 2$ and $EL = 1$ respectively, as shown in Figure 9(c)(d). If $EL = 0$, the histogram will be modified by the following criteria.

$$s''_k(i, j) = \begin{cases} s'_k(i, j) + (-1)^{q+1} & \text{if } d_k(i, j) = 0, w = 1 \\ s'_k(i, j) & \text{if } d_k(i, j) = 0, w = 0 \end{cases} \quad (5)$$

Where $1 \leq k \leq u \times v, k \neq m$ and q denotes the q th encountered $s_k(i, j)$ equaling $s_m(i, j)$ ($k \neq m$).

3) Type II-2

If $EL > 0$, the secret bit is embedded by repeating $EL = 2$ and $EL = 1$ respectively, as shown in Figure 9(c)(d). If $EL = 0$, the histogram will be modified by the following criteria.

$$s''_k(i, j) = \begin{cases} s'_k(i, j) - 1 & \text{if } d_k(i, j) = 0, w = 1, q < n_r - n_l \\ s'_k(i, j) + (-1)^{q+1} & \text{if } d_k(i, j) = 0, w = 1, q \geq n_r - n_l \\ s'_k(i, j) & \text{if } d_k(i, j) = 0, w = 0 \end{cases} \quad (6)$$

Where $1 \leq k \leq u \times v, k \neq m$ and q denotes the q th encountered $s_k(i, j)$ equaling $s_m(i, j)$ ($k \neq m$).

4) Type II-3

If $EL > 0$, the secret bit is embedded by repeating $EL = 2$ and $EL = 1$ respectively, as shown in Figure 9(c)(d).

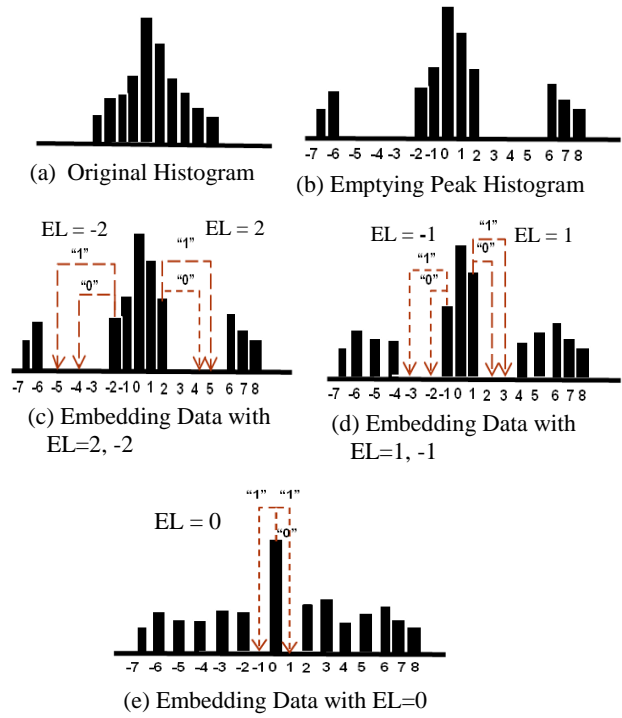


Figure 9: Exmple of data embedding

If $EL = 0$, the histogram will be modified by the following criteria.

$$s''_k(i, j) = \begin{cases} s'_k(i, j) + 1 & \text{if } d_k(i, j) = 0, w = 1, q \leq n_r - n_l \\ s'_k(i, j) - (-1)^{q+1} & \text{if } d_k(i, j) = 0, w = 1, q > n_r - n_l \\ s'_k(i, j) & \text{if } d_k(i, j) = 0, w = 0 \end{cases} \quad (7)$$

Where $1 \leq k \leq u \times v, k \neq m$ and q denotes the q th encountered $s_k(i, j)$ equaling $s_m(i, j)$ ($k \neq m$).

Step 8. Difference computation

In this step, the subimages $s''_1, s''_2, \dots, s''_{u \times v}$ are recomposed as the marked image I' .

B. Data Extraction

Data extraction process is a reverse process of data embedding.

4 Conclusion

In this paper, we have provided a detailed data hiding on medical images. Reversible data hiding techniques have been widely used among medical imaging systems. However, most of the methods are testing on 8-bit depth medical images with intensity levels from 0 to 255. Many high quality medical devices output with great precision

images such as 16-bit depth images, since 8-bit depth medical images present 256 discrete intensity levels, which is hard to express the complicate anatomical structures and more duplicated values of intensity demonstrate in medical images. Therefore, data hiding techniques with high quality images will be the important issues in the future works.

Acknowledgments

We would like to thank National Cancer Institute for providing the CT image data used in this study.

References

- [1] W. Bender, D. Gruhl, N. Morimoto, and A. Lu, "Techniques for data hiding", IBM System Journal, vol. 35, pp. 313-336, 2003.
- [2] Z. Chang and J. Xu, "Reversible run length data embedding for medical images," Communication Software and Networks (ICCSN), 2011 IEEE 3rd International Conference, pp. 260-263, 2011.
- [3] C. C. Chang, P. Y. Pai, C. M. Yeh, and Y. K. Chan, "A high payload frequency-based reversible image hiding method," Information Sciences, vol.180, pp. 2286-2298, 2010.
- [4] C. C. Chang, W. L. Tai, and K. N. Chen, "Lossless data hiding based on histogram for image authentication," IEEE/IFIP International Conference on Embedded and Ubiquitous Computing, pp. 506-511, 2008.
- [5] C. C. Chang, C. C. Lin, C. S. Tseng, W. L. Tai, "Reversible hiding in DCT-based compressed images," Information Sciences, vol. 177, no. 13, pp. 2768-2786, 2007.
- [6] C. C. Chang, C. C. Lin, Y. H. Fan, "Lossless data hiding for color images based on block truncation coding," Pattern Recognition, vol. 41, pp. 2347-2357, 2008.
- [7] S. F. Chiou, I E. Liao, and M. S. Hwang, "A capacity-enhanced reversible data hiding scheme based on SMVQ", Imaging Science Journal, vol. 59, no. 1, pp. 17-24, Feb. 2011.
- [8] S. F. Chiou, I E. Liao, and M. S. Hwang, "A capacity-enhanced reversible data hiding scheme based on SMVQ", Imaging Science Journal, vol. 59, no. 1, pp. 17-24, Feb. 2011.
- [9] Digital Imaging and Communications in Medicine. Available at <http://medical.nema.org/>.
- [10] M. Fallahpour, D. Megias, and M. Ghanbari, "Reversible and high-capacity data hiding in medical images," IET Image Process, vol. 5, Iss. 2, pp. 190-197, 2011.
- [11] J. B. Feng, I. C. Lin, C. S. Tsai, and Y. P. Chu, "Reversible watermarking: Current status and key issues," International Journal Network Security, vol. 12, no. 3, pp. 161-171, 2006.
- [12] H. Huang and W. Fang, "Integrity preservation and privacy protection for medical images with histogram-based reversible data hiding", Life Science System and Applications Workshop, pp. 108-111, 2011.
- [13] D. C. Lou, M. C. Hu, and J. L. Liu, "Multiple layer data hiding scheme for medical images," Computer Standards and Interfaces, vol. 31, pp. 329-335, 2009.
- [14] H. Luo, F. X. Yu, H. Chen, Z. L. Huang, H. Li, and P. H. Wang, "Reversible data hiding based on block median preservation," Information Sciences, vol. 181, pp. 308-328, 2011.
- [15] C. C. Lin, S. P. Yang, and N. L. Hsueh, "Lossless data hiding based on difference expansion without a location map," Congress on Image and Signal Processing, pp. 8-12, 2008.
- [16] D. C. Lou, M. C. Hu, J. L. Liu, "Multiple layer data hiding scheme for medical images," Computer Standard and Interfaces, vol 31, pp. 329-335, 2009.
- [17] Z. Ni, Y. Q. Shi, N. Ansari, W. Su, Q. Sun, and X. Lin, "Robust lossless image data hiding designed semi-fragile image authentication," IEEE Transactions on Circuits and Systems for Video Technology, vol. 18, no. 4, pp. 497-509, 2008.
- [18] Z. Ni, Y. Q. Shi, N. Ansari, and W. Su, "Reversible data hiding," IEEE Transactions on Circuits and Systems for Video Technology, vol. 16, pp. 354-362, 2006.
- [19] National Cancer Imaging Archive. Available at <https://imaging.nci.nih.gov/>.
- [20] M. Rochan, S. Hariharan, and K. Rajamani, "Data hiding scheme for medical images using lossless code for mobile HIMS," Third International Conference on Communication Systems and Networks, pp. 1-4, 2011.
- [21] D. B. Satre and R. V. Pawar, "Preserve robustness for image data hiding," Second International Conference on Computer Research and Development, pp. 707-711, 2010.
- [22] J. Tian, "Reversible data embedding using a difference expansion," IEEE Transactions on Circuits and Systems for Video Technology, vol. 13, no 8, pp. 890-896, Aug. 2003.
- [23] M. H. Tsai, S. F. Chiou, and M. S. Hwang, "A progressive image transmission method for 2D-GE image based on context feature with different thresholds", International Journal of Innovative Computing, Information and Control, vol. 5, no. 2, pp. 379-386, Feb. 2009.
- [24] C. D. Vleeschouwer, J. F. Deloagle, and B. Macq, "Circular interpretation of bijective transformation in lossless watermarking for media asset management," IEEE Transactions on Multimedia, vol. 5, pp. 97-105, 2003.
- [25] W. J. Wang, C. T. Huang, and S. J. Wang, "VQ applications in steganographic data hiding upon multimedia images," IEEE Systems Journal, vol. 5, no. 4, pp. 528-537, 2011.
- [26] C. C. Wu, S. J. Kao, and M. S. Hwang, "A high quality image sharing with steganography and adaptive authentication scheme", Journal of Systems and Software, vol. 84, no. 12, pp. 2196-2207, 2011.

[27] C. C. Wu, M. S. Hwang, and S. J. Kao, "A new approach to the secret image sharing with steganography and authentication", *Imaging Science Journal*, vol. 57, no. 3, pp. 140-151, June 2009.

Li-Chin Hwang received the B.S. and M.S. in Information Management from Chaoyang University of Technology (CYUT), Taichung, Taiwan, in 2001 and in 2003. She is currently working toward the PhD degree in the Department of Computer Science and Engineering at the National Chung Hsing University (NCTU), Taiwan. Her current research interests include information security, cryptography, medical image, and mobile communications.

Lin-Yu Tseng received the B.S. degree in mathematics from the National Taiwan University, in 1975, the M.S. degree in computer science from the National Chiao Tung University, Taiwan, in 1978, and the Ph.D. degree in computer science from National Tsing Hua University, Taiwan, in 1988. He is presently a Professor in the Department of Computer Science and Communication Engineering, Providence University, Taiwan. His research interests include evolutionary computation, neural network, multimedia systems, image processing, pattern recognition, and bioinformatics.

Min-Shiang Hwang received the B.S. in Electronic Engineering from National Taipei Institute of Technology, Taipei, Taiwan, ROC, in 1980; the M.S. in Industrial Engineering from National Tsing Hua University, Taiwan, in 1988; and the Ph.D. in Computer and Information Science from National Chiao Tung University, Taiwan, in 1995. He also studied Applied Mathematics at National Cheng Kung University, Taiwan, from 1984-1986. Dr. Hwang passed the National Higher Examination in field "Electronic Engineer" in 1988. He also passed the National Telecommunication Special Examination in field "Information Engineering", qualified as advanced technician the first class in 1990. He was a chairman of the Department of Information Management, Chaoyang University of Technology (CYUT), Taiwan, during 1999-2002. He is currently a professor of the department of Management Information System, National Chung Hsing University, Taiwan, ROC. He obtained 1997, 1998, 1999, 2000, and 2001 Outstanding Research Awards of the National Science Council of the Republic of China. He is a member of IEEE, ACM, and Chinese Information Security Association. His current research interests include electronic commerce, database and data security, cryptography, image compression, and mobile computing. Dr. Hwang had published 170+ articles on the above research fields in international journals.